Rate of chaotic mixing and boundary behavior

Rob Sturman* and James Springham†
Department of Applied Mathematics, University of Leeds, Leeds, United Kingdom
(Received 6 April 2011; revised manuscript received 27 June 2012; published 14 January 2013)

We discuss rigorous results on the rate of mixing for an idealized model of a class of fluid mixing device. These show that the decay of correlations of a scalar field is governed by the presence of boundaries in the domain, and in particular by the behavior of the modeled fluid at such boundaries.

DOI: 10.1103/PhysRevE.87.012906   PACS number(s): 47.10.Fg, 47.51.+a, 47.52.+j

I. INTRODUCTION

The fundamental idea behind mixing by chaotic advection is to exploit the exponential stretching inherent in a chaotic dynamical system to mix fluid, again at an exponential rate [1]. The mechanisms underlying these dynamics, and their application to fluid mixing, are now well understood. However, the real-world picture is complicated by the introduction of necessary boundaries, which can slow the rate of mixing, as has been observed [2,3].

The literature contains several descriptions and analyses of the mechanisms behind this phenomenon, for example, [4–8]. These approaches are often based on strange eigenmodes and in particular the interplay between advection and diffusion. What is observed and investigated is that, instead of an exponential decay in scalar concentration variance, as one might expect from chaotic dynamics, the rate of decay is slowed to an algebraic rate by the behavior of the fluid at the walls of the domain. Of course, the variance of concentration represents just one diagnostic for characterizing the rate of a mixing process. In this article we describe new rigorous results from the field of smooth ergodic theory. These imply that for a simple prototype model of standard mixing devices, this behavior is exactly what is expected for the evolution of *any* scalar field, even in the absence of diffusive effects. Moreover, these results illuminate the mechanisms underlying the competition between chaotic advection and boundary behavior.

In ergodic theory, an invertible measure-preserving transformation f on a domain M (normalized to $\mu(M) = 1$) is defined to be *(strong) mixing* if for any pair of measurable sets A and B we have

$$\lim_{n\to\infty} \mu(f^n(A) \cap B) = \mu(A)\mu(B), \qquad (1)$$

where $\mu(\cdot)$ is the invariant measure. This has a natural interpretation for applications to fluid mixing, where for incompressible fluids the invariant measure is Lebesgue (that is, volume). A natural question is that of how quickly the limiting process reveals the asymptotic independence of the arbitrary sets A and B. Ergodic theory attempts to answer such a question through the study of the *decay of correlations*. Thus rather than inspecting the behavior of actual sets in the system, one considers a real-valued function (usually called an *observable*) on M. For a mixing process, the correlation between two typical observables (or between an observable and itself) decays to zero as mixing occurs, and this rate of decay may, in certain situations, be quantified with some precision. The significance for fluid mixing is that the observable functions may represent any typical laboratory measurement.

Many mixing devices fall into the category of blinking systems; devices in which a steady flow is made nonintegrable by introducing a time or spatial dependence. One classical and well-known model for such a scenario is the (Arnold) cat map [9], the canonical example of a *hyperbolic toral automorphism*. It is relatively straightforward to show that this transformation enjoys exponential decay of correlations, and several different methods can be used [10]. However, although this is an instructive model of chaotic dynamics, and has been used as a model in a fluid mixing situation [11–13], it fails to capture many details of any real mixing device. In particular, the cat map is defined on the torus and has no boundary conditions. Moreover, this transformation is linear, identical at every point, and uniformly hyperbolic. For all these reasons, the same methods used to prove the exponential decay of correlations cannot typically be translated into proofs of a similar property for real mixing devices.

Linked twist maps have been proposed as a prototype model for blinking flows [14–16]. While these are still idealizations of physical systems, they encapsulate more general behavior than the cat map. Most crucially for our purposes here is that they are nonuniformly hyperbolic, and possess a boundary at which particular fluid boundary conditions can be modeled. A linked twist map could be regarded as an archetype of nonuniform chaos (for different reasons to the system in Ref. [17]), in which the nonuniformity stems from a boundary region in which orbits get trapped, before being reinjected into a hyperbolic mixing region.

II. DEFINITION AND RELEVANCE OF A LINKED TWIST MAP

A linked twist map (LTM) can be defined on both the plane (making it an appropriate model for many duct flows and blinking flows), or on a torus (where it has also successfully modeled practical devices; see [14]). Here we give a full description of the toral version. Fix $x_0, x_1, y_0, y_1 \in [0,1]$ and on the torus $\mathbb{T}^2 = [0,1] \times [0,1]$ define a pair of annuli

$$P = \{(x,y) | y \in [y_0, y_1]\} \quad \text{and} \quad Q = \{(x,y) | x \in [x_0, x_1]\}.$$

*r.sturman@maths.leeds.ac.uk
†j.springham@leeds.ac.uk

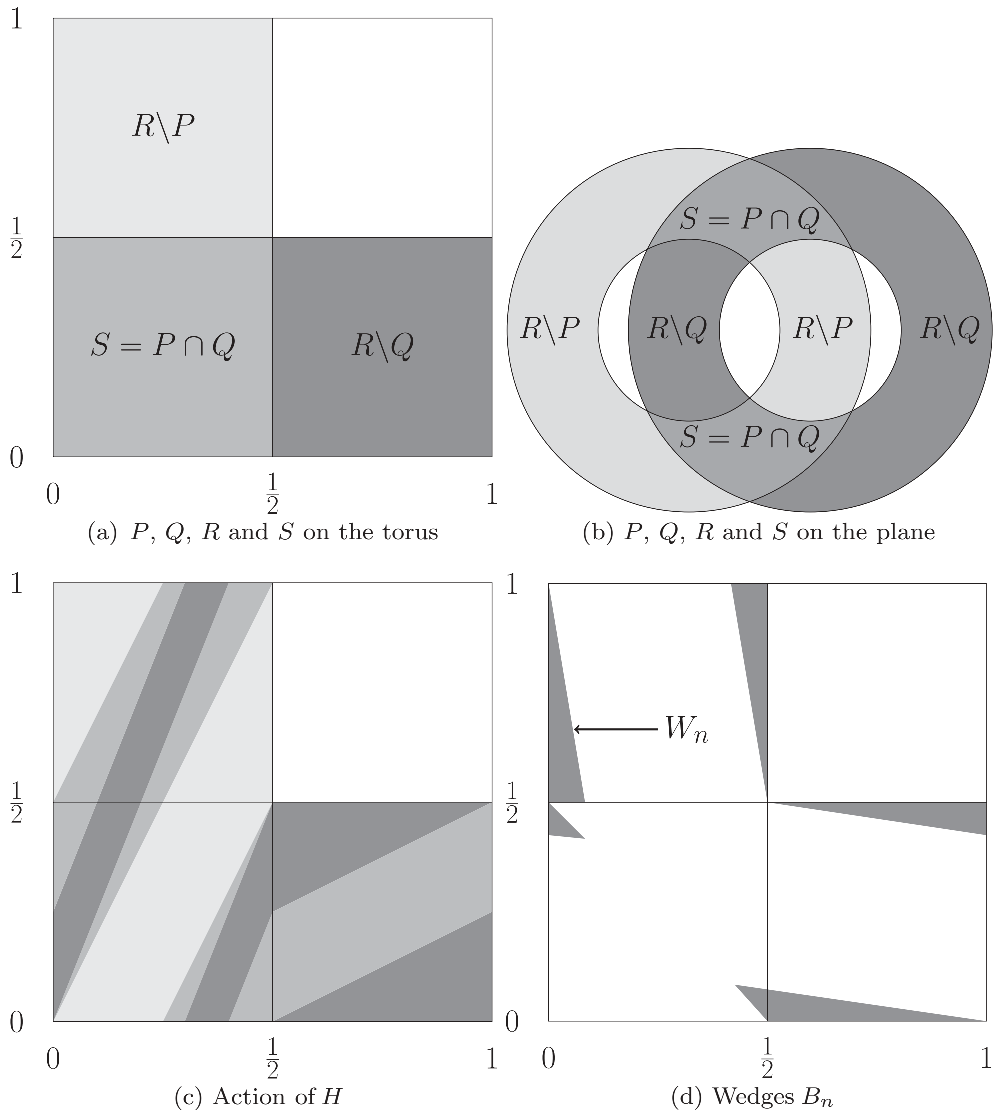

FIG. 1. (a) The torus $\mathbb{T}^2$ with $x_0 = y_0 = 0$, $x_1 = y_1 = \frac{1}{2}$. The set R is shaded: S is midgray, $R\backslash P$ is light gray, $R\backslash Q$ is dark gray; (b) the corresponding sets for a linked twist map on the plane; (c) the image of these shaded sets under $H = G \circ F$ with $k = l = 1$ and f and g linear. (d) The set B_n is shaded; for each n this set has a similar shape, the wedges becoming thinner with increasing n.

Denote $R = P \cup Q$ and $S = P \cap Q$. Define *twist maps* $F : P \to P$ and $G : Q \to Q$ by

$$F(x,y) = (x + f(y), y) \quad \text{and} \quad G(x,y) = (x, y + g(x)),$$

where $f : [y_0, y_1] \to \mathbb{R}$ is such that $f(y_0) = 0$, $f(y_1) = k$, an integer, and f is strictly monotonic. Similarly $g : [x_0, x_1] \to \mathbb{R}$ is such that $g(x_0) = 0$, $g(x_1) = l$, an integer, and g is strictly monotonic. Note that F and G leave invariant points on the boundaries of P and Q, respectively. This guarantees that the LTM is continuous. We let F be the identity map on $R\backslash P$ and G be the identity map on $R\backslash Q$. Both F and G are area-preserving. Consequently the *linked twist map* $H = G \circ F$, illustrated in Fig. 1, is an area-preserving transformation of R into itself.

In spite of its apparent simplicity (a composition of a pair of integrable shear maps), an LTM is a source of rich, and far from trivial, dynamical behavior. The map is nonuniformly hyperbolic; for details see Sturman *et al.* [14], and is mixing (that is, H satisfies Eq. (1), first shown by Wojtkowski [18]). Indeed it enjoys the Bernoulli property [19,20]; the system is statistically equivalent to an independent identically distributed random process. In this sense it possesses stronger ergodic mixing properties than mere mixing. However, this additional complexity itself does not imply anything about the rate at which correlations decay. Note that taking $x_0 = y_0 = 0$, $x_1 = y_1 = 1$, and $k = l = 1$ with f and g linear recovers the uniformly hyperbolic cat map.

Many fluid mixing devices operate with some periodicity, either spatial or temporal, and work on the basis of repeatedly shearing fluid first in one direction, and then in a transverse direction. The archetypal model behind many varied designs of mixer is the well known *blinking vortex* of Aref [21]. In such a scheme, a pair of point vortices are operated alternately, each rotating and shearing the fluid about a different stagnation point. The two spatial dimensions of such a Stokes flow, with the time-dependence of the alternating operation, allows the possibility of chaotic advection. The periodicity of the time-dependence means that discrete time maps such as F and G can be used to represent the dynamics of the continuous time fluid equations, where such maps are constructed as time-τ maps of a blinking flow, with τ the time between different flow patterns. In the LTM framework described above, replacing the toral annuli P and Q with interlinked planar annuli, with the pair of intersections now playing the role of S, and defining twist maps F and G on P and Q accordingly, as in Fig. 1(b), creates a suitable model for the blinking vortex system. A planar LTM can also be used to model a wider variety of mixing device, including pipe flows, such as the partitioned-pipe mixer [22], the rotated-arc mixer [23], and various electroosmotic flows [24,25], each of which have a spatial periodicity producing different cross-sectional flow patterns. An LTM is then constructed as the composition of maps defined by following the flow through each periodic element.

Although the torus may appear an unlikely domain for practical considerations, doubly periodic boundary conditions can be found in egg-beater flows [26,27] and also in mixers constructed from source–sink pairs, such as those described by the authors of [28–32].

III. QUANTIFYING THE RATE OF MIXING

The ergodic theory definition of mixing given by Eq. (1) can be written in the following equivalent functional form: H is mixing if the correlation function

$$C_n(\varphi,\psi) = \left| \int (\varphi \circ H^n)\psi\, d\mu - \int \varphi\, d\mu \int \psi\, d\mu \right|$$

tends to zero as $n \to \infty$ for any pair of bounded measurable functions φ and ψ. Moreover, the *rate* at which C_n approaches zero governs the rate at which the transformation mixes. A typical approach in ergodic theory is to choose a particular transformation H, and then prove a result concerning such a rate for a wide class of observable functions φ and ψ. In fact, it is usual to consider all observables which have sufficient regularity; for example, all Hölder continuous functions. Note that arbitrarily slow decay can be achieved for observables with no regularity properties. Such a result then certainly allows one to establish information for a particular scalar observable, such as concentration.

Let $\mathcal{H}_\alpha$ denote the space of real-valued, α-Hölder functions on R, that is, the functions $\varphi : R \to \mathbb{R}$ for which there is $C > 0$ such that for all $z,z' \in R, |\varphi(z) - \varphi(z')| \leqslant C d(z,z')^\alpha$, where $d(\cdot,\cdot)$ denotes distance on R. We restrict (without loss of generality) to the case in which the observable ψ has zero average, and so study the rate of decay as $n \to \infty$ of

$$C_n(\varphi,\psi) = \int_R (\varphi \circ H^n)\psi\, d\mu. \tag{2}$$

IV. EFFECT OF THE BOUNDARY

An appealing feature of linked twist maps is that the source of both the hyperbolicity *and* the nonuniformity of that hyperbolicity are quite apparent. In the following we consider a particular LTM with $x_0 = y_0 = 0$, $x_1 = y_1 = 1/2$, $f(y) = 2y$ and $g(x) = 2x$, as in Fig. 1. As frequently occurs in a typical trajectory, if $z \in P$ and $F(z) \in S$ then the derivative

$$DH = DG \cdot DF = \begin{pmatrix} 1 & 0 \\ 2 & 1 \end{pmatrix} \begin{pmatrix} 1 & 2 \\ 0 & 1 \end{pmatrix} = \begin{pmatrix} 1 & 2 \\ 2 & 5 \end{pmatrix}$$

is a hyperbolic matrix. This is the source of hyperbolicity, and corresponds in a real device to a region of fluid stretched first in one direction and then another by a blinking flow. Any trajectory of H which lands nowhere other than S experiences precisely this hyperbolicity at each iterate. Such a trajectory is then uniformly hyperbolic, with the Lyapunov exponents equal to the logarithms of the eigenvalues of DH. However, initial conditions producing trajectories with this property form a set of zero measure in R.

For almost all trajectories, it often happens instead that one of F,G is the identity (for example, for $z \in R\backslash P$) in which case DH is nonhyperbolic. This may be the case for an arbitrary number of successive images of z (see the "wedges" defined below), diluting the growth of tangent cones with each iteration. The effect is that Lyapunov exponents are still nonzero, but are not uniformly bound away from zero.

Our motivation in this section is the presumption that the same regions of R that impede the hyperbolicity of H also impede its mixing. With this in mind we study the contribution to the correlation function C_n arising from the domain

$$B_n = \{z \in R : H^n(z) = F^n(z) \text{ or } H^n(z) = G^n(z)\}.$$

These sets contains those points which stick close to the boundary for n steps before entering the hyperbolic region. These can also be thought of as those points which form "regions of low stretching [which] slow down mixing and contaminate the whole mixing pattern ..." [33]. It is an easy exercise to deduce that B_n consists of four connected components, each having the form of a "wedge." These are illustrated in Fig. 1(d). The fixed order of composition $G \circ F$ leads to a lack of symmetry between those wedges contained in Q and those contained in P.

Although it is difficult in general to compute C_n exactly, we discuss here the contribution to this integral of the region B_n. We first restrict our attention to one of the wedges, denoted W_n, being in Q and having as a boundary the line $x = 0$ [shown in Fig. 1(d)]. This is because the dynamics on W_n are effectively the same as those on the other components of B_n. Its other boundaries satisfy $y = 1/2$ and $x = (1 - y)/2n$, respectively. Consider

$$I_n = \int_{W_n} (\varphi \circ H^n)\psi\, d\mu.$$

We show that $I_n \sim K'/n$ for some (generally nonzero) K' and that the same holds for the three remaining wedges constituting $B_n\backslash W_n$. Here we use $\sim$ to indicate the common asymptotic notation given by $f \sim g$ if $f/g \to 1$ for functions f and g. We remark that $\mu(W_n) = \mathcal{O}(1/n)$ and the observables are bounded, so it is trivial that an upper bound on the integral should have this form. We are arguing that the decay rate is no faster than this.

By definition if $z = (x,y) \in W_n$ then $H^n(x,y) = G^n(x,y) = (x, y + 2nx)$ so that I_n can be written explicitly as

$$I_n = \frac{4}{3} \int_{\frac{1}{2}}^{1} \int_{0}^{(1-y)/2n} \varphi(x, y + 2nx)\psi(x,y)\, dx\, dy,$$

where we have used $\int dxdy = \frac{3}{4}\int d\mu$. To estimate I_n consider the related double integral

$$J_n = \frac{4}{3}\int_{\frac{1}{2}}^{1}\int_{0}^{(1-y)/2n} \varphi(0,y+2nx)\psi(0,y)dxdy.$$

This integral differs from I_n in that the integrand is evaluated along the boundary $x=0$ rather than at all points in W_n. Making the substitution $t = y + 2nx$ we have

$$J_n = \frac{2}{3n}\int_{\frac{1}{2}}^{1}\psi(0,y)\int_{y}^{1}\varphi(0,t)dtdy.$$

The substitution clarifies the nature of the n-dependence of J_n. The double integral is now simply a constant which depends only on the functions φ and ψ, and so in particular we have $J_n \sim K_1/n$ for some constant K_1 depending only on the values of φ and ψ at the boundary.

The desired result then follows if we establish that $\lim_{n\to\infty} n|I_n - J_n| = 0$ (that is, that the two integrals I_n and J_n are sufficiently close). The significance of this statement is that the contribution made to the correlation function by points *near* the boundary is asympotically the same as the contribution made by points *at* the boundary. Consider

$$n|I_n - J_n| = \frac{4n}{3}\left|\int_{\frac{1}{2}}^{1}\int_{0}^{(1-y)/2n}\varphi(x,t)\psi(x,y) - \varphi(0,t)\psi(0,y)dxdy\right| \to 0$$

as $n\to\infty$. We retain the notation $t = y + 2nx$ for convenience. The domain of integration is $\mathcal{O}(1/n)$ and so it is enough to show that the integrand approaches zero as $n\to\infty$. Indeed the integrand is bounded above in absolute value by

$$\begin{aligned}&|\varphi(x,t)|\,|\psi(x,y)-\psi(0,y)| + |\psi(0,y)|\,|\varphi(x,t)-\varphi(0,t)|\\ &\leqslant \varphi_{\max}|x|^{\alpha} + \psi_{\max}|x|^{\alpha}\\ &\leqslant \text{const}\, n^{-\alpha}.\end{aligned}$$

For the first bound we have used the α-Hölder property and used $\varphi_{\max}$ and $\psi_{\max}$ to denote the suprema of φ and ψ on R. For the second bound we have used $|x| \leqslant 1/2(n-1)$ on W_n. This completes the proof that $I_n \sim K'/n$; the case of the other wedge in Q is entirely similar.

Now suppose that W_n' is a wedge in P and, without loss of generality, that $y=0$ is a boundary of W_n'. Geometrically W_n' is a little different to W_n since the first occurrence of F removes W_n' from S. Using the boundedness of φ and ψ, and the fact that $1/2(n+1) - 1/2n = \mathcal{O}(1/n^2)$ we have

$$\begin{aligned}&\int_{W_n'}(\varphi\circ H^n)\psi d\mu\\ &= \frac{4}{3}\int_{\frac{1}{2}}^{1}\int_{0}^{(1-x)/2n}\varphi(x+2ny,y)\psi(x,y)dydx + \mathcal{O}\left(\frac{1}{n^2}\right).\end{aligned}$$

The result follows in the same manner as above since the leading order term is again $\mathcal{O}(1/n)$.

It follows immediately that

$$C_n \sim \frac{K}{n} + \int_{R\backslash B_n}(\varphi\circ H^n)\psi d\mu.$$

V. DECAY OF CORRELATIONS FOR LTMs

Computing the contribution of $R\backslash B_n$ to C_n is rather more difficult. *A priori* there may be some other subregion of R which contributes at an even slower rate to the decay of C_n, and hence dominates. This in fact cannot happen [34]. The proof appeals to the seminal work of Young [35,36]. To apply these results directly, one needs to construct a region Λ with *hyperbolic product structure* and study the return times to Λ. An instructive example is given by Chernov and Young [37], in which Λ is described explicitly for the uniformly hyperbolic cat map. It may be tempting to assume here that S should suffice as the hyperbolic region Λ, but matters are more complicated for LTMs. An intuitive reason for this is that local stable and unstable manifolds do not exist everywhere (only μ-almost everywhere) and so Λ, defined as an intersection of such manifolds, cannot be simply connected (i.e., it must contain holes). This immediately rules out simply-connected sets such as S as candidates for Λ. In general, for nonuniformly hyperbolic systems, the explicit construction of Λ is typically prohibitively difficult. The work of Chernov [38] and Chernov and Zhang [39] gives a method to obtain conclusions related to those of Young while not explicitly constructing Λ. Instead, one finds a region Y, such that $\Lambda\subset Y$, in which hyperbolicity is sufficiently strong, and some other technical conditions are satisfied (in particular, the interplay between the hyperbolicity of the system and the singularities generated from images of the boundaries of P and Q). Here S can be taken as the choice of Y. Finally to reach the conclusions of Young from those of Chernov we appeal to a result of Markarian [40], which involves considering in detail a certain set of points which return to S particularly infrequently.

The work briefly discussed in the preceding paragraph has been completed by the present authors and can be found in Springham and Sturman [34], and so we have the rigorous conclusion that correlations for LTMs decay at a rate no slower than $C_n = \mathcal{O}(1/n)$. Moreover, the argument of Sec. IV shows that this bound is optimal, providing the following two conditions hold.

First, that the contributions from each wedge do not cancel each other out. Note that it would be possible to choose observable functions with a symmetry between the wedges of B_n to achieve this cancellation. Avoiding such observables is straightforward, and indeed generic.

Second, that the decay rate of $\int_{R\backslash B_n}(\varphi\circ H^n)\psi d\mu$ is, to leading order, not precisely equal to $-K/n$, thus again canceling out the $\mathcal{O}(1/n)$ decay rate and allowing a faster decay of correlations. Once more the result stands providing such a pathological choice of observables is not taken.

VI. MORE GENERAL BOUNDARY BEHAVIOR

We now consider perturbations of the twists f and g that are nonlinear in a neighborhood of the boundary. Fix $p>0$, $0<\varepsilon\ll\frac{1}{4}$ and for $x,y\in[0,\varepsilon)\cup(\frac{1}{2}-\varepsilon,\frac{1}{2}]$ let

$$\tilde{F}(x,y) = (x+2y^p,y) \quad\text{and}\quad \tilde{G}(x,y) = (x,y+2x^p) \qquad (3)$$

and consider the LTM $\tilde{H} = \tilde{G}\circ\tilde{F}$. Note that we do not prescribe the form of the twist maps away from this region (other than to insist on their monotonicity as before), but simply concentrate on the behavior near the boundary. Such functions can represent different possible boundary layer behavior in a fluid situation.

Defining B_n as before we claim that there exists $K_p = K_p(\varphi,\psi) \in \mathbb{R}$, in general nonzero, so that

$$\int_{B_n} (\varphi \circ \tilde{H}^n)\psi \, d\mu \sim \frac{K_p}{n^{1/p}}. \tag{4}$$

The claim is established just as in Sec. IV; only minor changes are required so we omit a proof. This result implies that the linked twist map just described experiences decay of correlations at the polynomial rate $n^{-1/p}$.

Other recent studies have also noted the role of material near to walls in mixing problems ("peripheral regions" in Chertkov and Lebedev [6], Lebedev and Turitsyn [7], Chernykh and Lebedev [8], "parabolic periodic points" in Gouillart *et al.* [41]). In Lebedev and Turitsyn [7], a distinction is made between decay rates in vessels and pipes. In particular, the mathematical models therein use incompressibility to derive boundary layer behavior in the peripheral regions. In the vessel case, the velocity component perpendicular to the wall $v_\perp$ scales as ϵ^2, where ϵ is the distance from the wall, while in the pipe case, $v_\perp$ scales as ϵ. This difference in boundary behavior is manifested in a difference in decay rates, which scale as $t^{-1/2}$ for the vessel (where t is time), and as z^{-1} for the pipe, where z is the coordinate along the pipe. These results are obtained by predicting the thickness of the boundary layer of unmixed fluid.

In the present paper, by contrast, area-preservation (corresponding to incompressibility) determines that there is no motion perpendicular to the walls. Instead, the size of the wedges B_n (corresponding to the thickness of the boundary layer) diminishes at a rate governed by the value of p as defined above. Thus the results herein are quite compatible with those

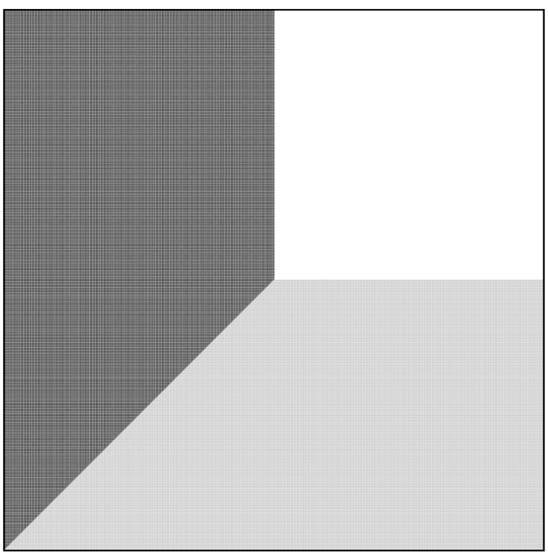

(a) Initial conditions

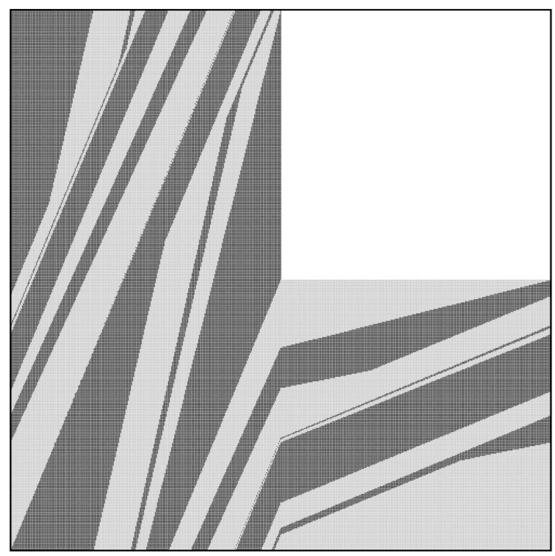

(b) After 2 iterates

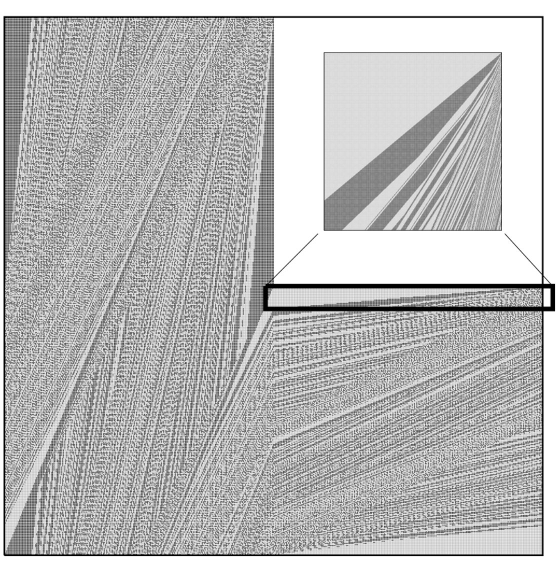

(c) After 6 iterates

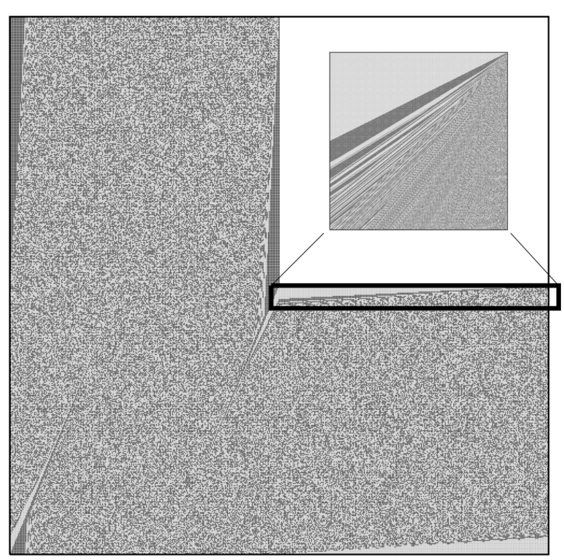

(d) After 10 iterates

FIG. 2. (a) Two initially segregated sets are iterated under the LTM H and shown after (b) 2, (c) 6, and (d) 10 iterates. In the latter two figures the empty square $\mathbb{T}^2 \backslash R$ is used to enlarge part of the domain contributing to the slowest mixing.

of Lebedev and Turitsyn [7] and Chernykh and Lebedev [8], with $p = 2$ representing the vessel case, and $p = 1$ modeling the pipe flow.

VII. NUMERICAL VERIFICATION

We illustrate the rigorous results above with the following simple numerical experiments. We seed the LTM with the initial conditions colored black if $x < y$ and gray if $x \geqslant y$ as shown in Fig. 2(a). Note that the upper right corner of the square (torus) plays no role. The images of these sets of initial conditions after 2, 6, and 10 iterations of the map H are shown in Figs. 2(b)–2(d). It is a simple matter to compute, for example, the maximum striation width for such a map, given by the perpendicular height of the wedges. Measuring striation width in a fluid mixing experiment is a common way to characterize the quality of a mixture, although the present theorems hold whichever method of quantifying the mixing process is chosen. This scales with n as $1/n$, as predicted by the discussion of Sec. IV. These widths are shown in Fig. 3(d) as circles, the fitted solid straight line A/n on the logarithmic plot indicating the algebraic decrease in maximum striation width.

We can support the statement of Eq. (4) by considering a related map. Here we replace the twist functions f and g with the functions

$$\tilde{f}(y) = 1 - \frac{\cos^{-1}(4y-1)}{\pi}, \quad \tilde{g}(x) = 1 - \frac{\cos^{-1}(4x-1)}{\pi},$$

which satisfy Eq. (3) near the boundaries with $p = 1/2$. In such a system points near the boundaries are sheared more

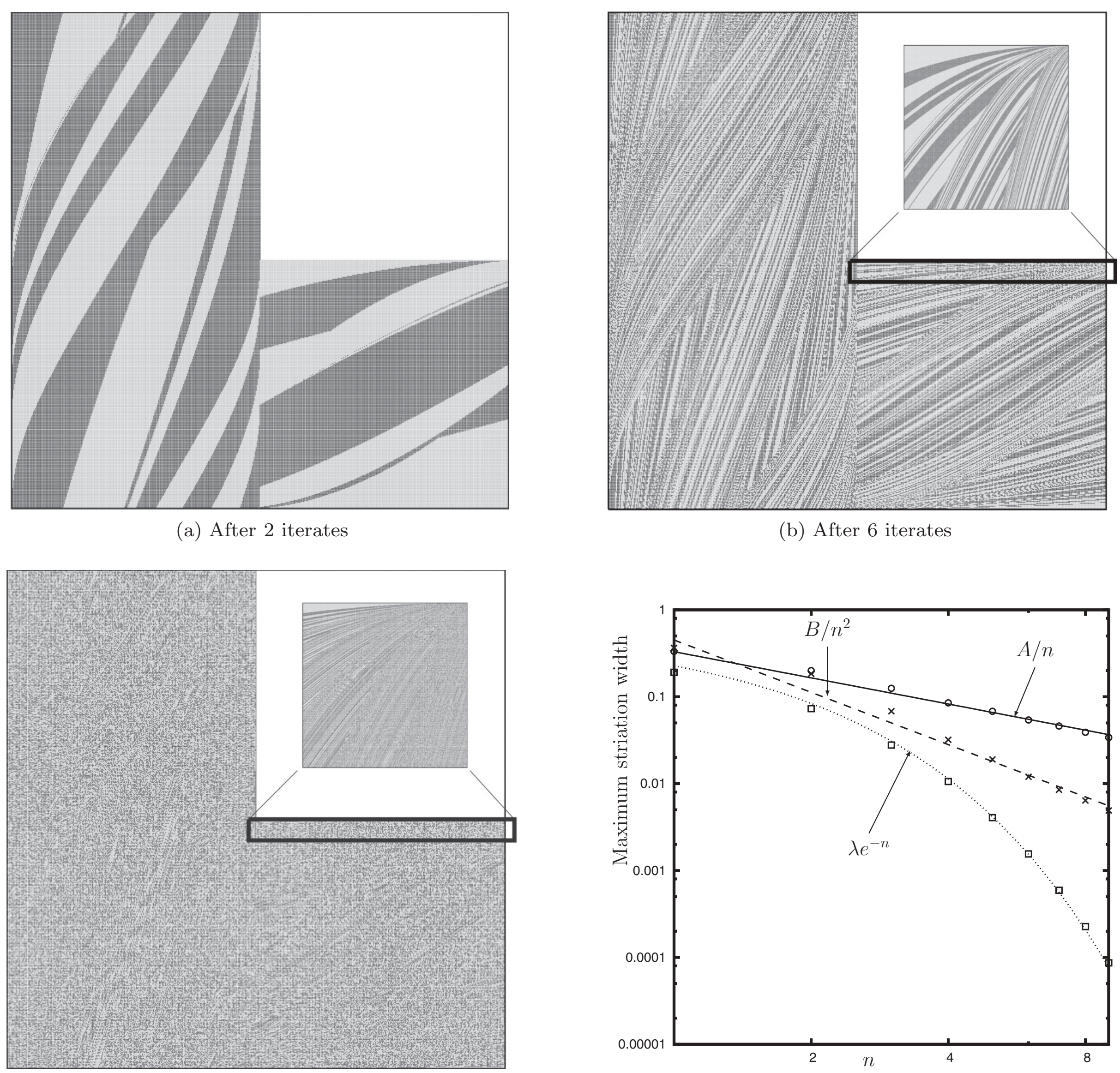

(a) After 2 iterates

(b) After 6 iterates

(c) After 10 iterates

(d) Width of largest striation

FIG. 3. The initial sets in Fig. 2 are iterated, under the nonlinear map $\tilde{H}$, (a) 2, (b) 6, and (c) 10 times. Relative to Fig. 2 the thickest striations, shown in the insets, are mixed more quickly, due to the particular behavior at the boundary. Panel (d) shows how the maximum striation width decreases with iteration, for the linear LTM (circles, solid line), the nonlinear LTM (crosses, dashed line), and the cat map (squares, dotted line).

strongly, representing boundary conditions in which points are moved more quickly at the walls. The resulting wedges of unmixed material are shrunk, and the maximum striation width reduced, plotted as crosses in Fig. 3(d) with dashed line B/n^2. This confirms that the striation width still decays algebraically, at a faster rate than for the linear case. For comparison, we include in Fig. 3(d) the width of the largest striation (plotted as squares) for the uniformly hyperbolic case identical to the above, but with $x_1 = y_1 = 1$ (i.e., the Arnold cat map). This has an exponential decay of correlations, and indeed these fit the dotted line given by λe^{-n}, where λ is the contracting Lyapunov exponent.

VIII. DISCUSSION AND CONCLUSION

Just as a hyperbolic toral automorphism provides a fundamental skeleton of two-dimensional area-preserving chaotic dynamics, so a linked twist map gives a nonuniform generalization which can form a paradigm model for chaotic dynamics with a boundary. Moreover, such maps underpin a wide class of fluid mixing device. Here we describe the results concerned with the rate of mixing of such maps. We give the main result which implies that the rate of decay of correlations is polynomial, rather than exponential, where the algebraic exponent depends on the boundary conditions of the domain. This provides an insight into the dynamical mechanism for a variety of recently reported experimental phenomena, in particular in the situation where advection dominates over diffusion.

The result of this paper is rigorous and general, but provides only a first order estimate on rates of mixing, and moreover applies to an idealized model of fluid mixing device. There are many natural avenues for further investigation, for example, what is the effect of adding diffusive effects to a linked twist map? An open question is that of higher order statistics for mixing behaviors. Lebedev and Turitsyn [7] and Chernykh and Lebedev [8], for example, described a complex situation in such details for mixing in vessels and pipes. One approach to this, related to the methods of the present paper and the subject of currently ongoing work, could be to study in greater detail the statistics of the return map to the hyperbolic region. Such a study for a single shear map has been made in Hu *et al.* [42], which also contains an analysis of return time distributions for systems with some mixing behavior. The corresponding result for linked twist maps is likely to be of significantly greater complexity.

ACKNOWLEDGMENTS

The authors thank Stephen Wiggins, Julio Ottino, Rich Lueptow, and Stefano Luzzatto, and anonymous referees for useful comments and conversations. This work was supported by the Leverhulme Trust Grant No. F/10101/A.

[1] J. M. Ottino, *The Kinematics of Mixing: Stretching, Chaos, and Transport* (Cambridge University Press, Cambridge, England, 1989).
[2] T. Burghelea, E. Segre, and V. Steinberg, Phys. Rev. Lett. **96**, 214502 (2006).
[3] C. Simonnet and A. Groisman, Phys. Rev. Lett. **94**, 134501 (2005).
[4] R. T. Pierrehumbert, Chaos Solitons Fractals **4**, 1091 (1994).
[5] E. Gouillart *et al.*, Phys. Rev. Lett. **99**, 114501 (2007).
[6] M. Chertkov and V. Lebedev, Phys. Rev. Lett. **90**, 034501 (2003).
[7] V. V. Lebedev and K. S. Turitsyn, Phys. Rev. E **69**, 036301 (2004).
[8] A. Chernykh and V. Lebedev, JETP Lett. **87**, 682 (2008).
[9] V. I. Arnold and A. Avez, *Ergodic Problems of Classical Mechanics* (Addison-Wesley, Boston, 1968).
[10] V. Baladi, in *Smooth Ergodic Theory and its Applications*, Proceedings of Symposia in Pure Mathematics, Vol. 69 (American Mathematical Society, Providence, 2001), pp. 297–325.
[11] H. Aref, Phys. Fluids **3**, 1009 (1991).
[12] B. Sundaram, A. C. Poje, and A. K. Pattanayak, Phys. Rev. E **79**, 066202 (2009).
[13] J.-L. Thiffeault and S. Childress, Chaos **13**, 502 (2003).
[14] R. Sturman, J. M. Ottino, and S. Wiggins, *The Mathematical Foundations of Mixing*, *Cambridge Monographs on Applied and Computational Mathematics*, Vol. 22 (Cambride University Press, Cambridge, England, 2006).
[15] J. M. Ottino and S. Wiggins, Philos. Trans. R. Soc. **362**, 923 (2004).
[16] J. M. Ottino and S. Wiggins, Science **305**, 485 (2004).
[17] S. Cerbelli and M. Giona, J. Nonlinear Sci. **15**, 387 (2005).
[18] M. Wojtkowski, in *Nonlinear dynamics*, Annals of the New York Academy of Sciences, Vol. 357 (Wiley, New York, 1980), pp. 65–76.
[19] F. Przytycki, Ann. Scient. Ec. Norm. Sup. **16**, 345 (1983).
[20] J. Springham and S. Wiggins, Dyn. Syst. **25**, 483 (2010).
[21] H. Aref, J. Fluid Mech. **143**, 1 (1984).
[22] D. V. Khakhar, J. G. Franjione, and J. M. Ottino, Chem. Eng. Sci. **42**, 2909 (1987).
[23] G. Metcalfe, M. Rudman, A. Brydon, and L. Graham, in *Proceedings of the 6th World Congress of Chemical Engineering* (Institution of Chemical Engineers, Melbourne, Australia, 2001).
[24] A. D. Stroock, M. Weck, D. T. Chiu, W. T. S. Huck, P. J. A. Kenis, and G. M. Whitesides, Phys. Rev. Lett. **84**, 3314 (2000).
[25] A. D. Stroock, S. K. W. Dertinger, A. Ajdari, I. Mezic, H. A. Stone, and G. M. Whitesides, Science **295**, 647 (2002).
[26] J. M. Ottino, Sci. Am. **260**, 56 (1989).
[27] J. G. Franjione and J. M. Ottino, Philos. Trans. R. Soc. London **338**, 301 (1992).
[28] M. A. Stremler and B. A. Cola, Phys. Fluids **18**, 011701 (2006).
[29] B. A. Cola, D. K. Schaffer, T. S. Fisher, and M. A. Stremler, J. Microelectromech. Syst. **15**, 259 (2006).
[30] M. K. McQuain, K. Seale, J. Peek, T. S. Fisher, S. Levy, M. A. Stremler, and F. R. Haselton, Anal. Biochem. **325**, 215 (2004).
[31] J. M. Hertzsch, R. Sturman, and S. Wiggins, Small **3**, 202 (2007).
[32] F. Raynal, F. Plaza, A. Beuf, P. Carrière, E. Souteyrand, J.-R. Martin, J. P. Cloarec, and M. Cabrera, Phys. Fluids **16**, L63 (2004).
[33] E. Gouillart *et al.*, Phys. Rev. E **78**, 026211 (2008).

[34] J. Springham and R. Sturman, arXiv:1212.0889 [Ergodic Theory and Dynamical Systems (to be published)].
[35] L.-S. Young, Ann. Math. **147**, 585 (1998).
[36] L.-S. Young, Isr. J. Math. **110**, 153 (1999).
[37] N. Chernov and L. S. Young, in *Hard Ball Systems and the Lorentz Gas*, *Encyclopaedia of Mathematical Sciences*, edited by D. Szasz, Vol. 101 (Springer, New York, 2000), pp. 89–120.
[38] N. Chernov, J. Stat. Phys. **94**, 513 (1999).
[39] N. Chernov and H. K. Zhang, Nonlinearity **18**, 1527 (2005).
[40] R. Markarian, Ergodic Theory Dyn. Syst. **24**, 177 (2004).
[41] E. Gouillart, O. Dauchot, B. Dubrulle, S. Roux, and J. L. Thiffeault, Phys. Rev. E **78**, 026211 (2008).
[42] H. Hu, A. Rampionni, L. Rossi, G. Turchetti, and S. Vaienti, Chaos **14**, 160 (2004).